

Available online at [www.sciencedirect.com](http://www.sciencedirect.com)

ScienceDirect

journal homepage: [www.e-jds.com](http://www.e-jds.com)

Original Article

# Cementocyte-derived extracellular vesicles regulate osteoclastogenesis and osteoblastogenesis

Jiajun Li <sup>a</sup>, Yukihiro Sakisaka <sup>a</sup>, Eiji Nemoto <sup>a\*</sup>,  
 Kentaro Maruyama <sup>a</sup>, Shigeki Suzuki <sup>a</sup>, Kaixin Xiong <sup>a</sup>,  
 Hiroyuki Tada <sup>b</sup>, Taichi Tenkumo <sup>c</sup>, Satoru Yamada <sup>a</sup>

<sup>a</sup> Division of Periodontology and Endodontology, Tohoku University Graduate School of Dentistry, Sendai, Japan

<sup>b</sup> Division of Oral Immunology, Tohoku University Graduate School of Dentistry, Sendai, Japan

<sup>c</sup> Division of Advanced Prosthetic Dentistry, Tohoku University Graduate School of Dentistry, Sendai, Japan

Received 29 January 2024; Final revision received 25 February 2024

Available online 2 March 2024

## KEYWORDS

Cementocytes;  
 Extracellular vesicles;  
 Osteoclasts;  
 Osteoblasts;  
 RANKL

**Abstract** *Background/purpose:* Cementum shares many properties with bone; however, in contrast to bone, it is not innervated or vascularized and has a limited capacity for remodeling. Osteocytes located in the lacunae-canalicular system of bone tissue play a central role in bone remodeling by communicating with osteoblasts and osteoclasts. Although cementocytes are present in cellular cementum and are morphologically similar to osteocytes, it remains unclear whether they are involved in the dynamic functional regulation of metabolism in cementum. The present study focused on the extracellular vesicles (EVs) secreted by cementocytes and examined their effects on osteoclasts and osteoblasts.

*Materials and methods:* EVs were extracted from the mouse cementocyte cell line, IDG-CM6. The effects of EVs on recombinant RANKL-induced osteoclastogenesis and recombinant Bone morphogenetic protein (BMP)-2-mediated osteoblastogenesis were investigated using the mouse osteoclast progenitor cell line, RAW264.7 and mouse pre-osteoblast cell line, MC3T3-E1, respectively.

*Results:* EVs enhanced the formation of tartrate-resistant acid phosphatase activity-positive cells. Real-time PCR revealed that EVs up-regulated the expression of osteoclast-related genes. On the other hand, the cell culture supernatant of cementocytes significantly inhibited the differentiation of osteoclasts. Regarding osteoblastogenesis, EVs suppressed the expression of alkaline phosphatase, bone sialoprotein, and osteocalcin induced by recombinant BMP-2 at the gene and protein levels.

\* Corresponding author. Department of Periodontology and Endodontology, Tohoku University Graduate School of Dentistry, 4-1 Seiryomachi, Aoba, Sendai 980-8575, Japan.

E-mail address: [e-nemoto@dent.tohoku.ac.jp](mailto:e-nemoto@dent.tohoku.ac.jp) (E. Nemoto).

**Conclusion:** A network of cementocytes, osteoblasts, and osteoclasts may exist in cellular cementum, which suggests the involvement of cementocytes in dynamic metabolism of cementum through EVs.

© 2024 Association for Dental Sciences of the Republic of China. Publishing services by Elsevier B.V. This is an open access article under the CC BY-NC-ND license (<http://creativecommons.org/licenses/by-nc-nd/4.0/>).

## Introduction

Cementum shares many properties with bone and has a similar biochemical composition, particularly the contents of the extracellular matrix. However, in contrast to bone, cementum is not innervated or vascularized and has a limited capacity for remodeling.<sup>1,2</sup> Cementum is classified as acellular cementum and cellular cementum depending on the presence or absence of cementocytes. During the formation of cellular cementum, cementoblasts located on the surface of cementum secrete a layer of an uncalcified extracellular matrix, a cementoid matrix. As the deposition of the cementoid matrix progresses, some cementoblasts become embedded in the cementoid matrix and become cementocytes. Osteocytes are terminally differentiated bone cells located in the bone lacunae of the bone matrix and are characterized morphologically by numerous dendritic processes. Dendrites communicate between adjacent bone canaliculi and the bone surface in order to interact with each other and with osteoblasts located on the bone surface. They form cellular networks in bone tissue, together with communication between osteocytes and distant cells via humoral factors.<sup>3,4</sup> Osteocytes play a central role in the regulation of bone remodeling.<sup>3,4</sup> Cementocytes are osteocyte-like cells that reside in the cementum lacunae of cellular cementum, which correspond to bone lacunae. Morphological studies demonstrated that dendrites extend through the canalicular system, maintaining gap junctions between neighboring cementocytes,<sup>5–7</sup> implying that cementocytes have similar functions to osteocytes in bone tissue. However, it remains unclear whether cementocytes are involved in the dynamic role of metabolism in cementum, i.e., the formation of cementum or the regulation of local osteoclast functions, equivalent to that of osteocytes.

A recent study reported that extracellular vesicles (EVs) are involved in many biological events.<sup>8</sup> EVs are membrane vesicles of 30–1000 nm in diameter that are secreted by most cells and contain large amounts of signaling molecules, such as proteins, lipids, mRNA, micro-RNA, and non-coding RNA. Furthermore, the profile of signaling molecules in EVs is highly dependent on the cell type and the physiological and pathological conditions of the cell.<sup>8</sup> The transfer of these molecules in EVs between cells controls many biological functions, and this information has contributed to rapid advances in our understanding of previously unresolved physiological functions, such as cardiac remodeling,<sup>9</sup> airway remodeling,<sup>10</sup> bone remodeling,<sup>11,12</sup> and tissue repair,<sup>13</sup> as well as pathological processes, including inflammation/anti-inflammation.<sup>14,15</sup> Recent studies showed that EVs released from periodontal

ligament cells in mechanical stress environments provided feedback to the inflammatory response of periodontal tissues,<sup>16</sup> osteocyte-derived EVs induced by mechanical stretch force promoted periodontal ligament cell proliferation and osteogenic differentiation,<sup>17</sup> and gingival tissue mesenchymal stem cell-derived EVs promoted the conversion of M1 macrophages to M2 macrophages.<sup>18</sup> These findings suggest that EVs play important roles in maintaining periodontal tissue homeostasis. However, few studies have investigated the involvement of EVs in cementum biology.

Therefore, the present study focused on EVs secreted by cementocytes and examined their effects on osteoclasts and osteoblasts.

## Materials and methods

### Reagents

Recombinant mouse receptor activator of nuclear factor- $\kappa$  B ligand (rRANKL), mouse interferon gamma (rIFN- $\gamma$ ), and mouse Wnt3a (rWnt3a) were purchased from PeproTech (Rocky Hill, NJ, USA). Exoquick-TC™ was obtained from System Biosciences LLC (Palo Alto, CA, USA). Recombinant human bone morphogenetic protein-2 (rBMP-2) was supplied by R&D Systems Inc. (Minneapolis, MN, USA). Ascorbic acid and  $\beta$ -glycerophosphate were from Sigma-Aldrich (St. Louis, MO, USA).

### Cell lines and cell culture

A murine cementocyte-like cell line (IDG-CM6) was obtained from Kerfast (Boston, MA, USA). These cells were maintained in  $\alpha$ -Minimum Essential Medium ( $\alpha$ -MEM) (Gibco™/Life Technologies, Carlsbad, CA, USA) with 10% heat-inactivated fetal bovine serum (FBS; Gibco™/Life Technologies), 100 U/ml penicillin G, and 100  $\mu$ g/ml streptomycin. This medium is referred to as complete  $\alpha$ -MEM. Cell culture dishes were coated with 0.15 mg/ml rat tail type I collagen (Atelo Cell® KOKEN Co., Tokyo, Japan). To induce the proliferation, cells were incubated with a complete  $\alpha$ -MEM supplemented with 50 U/ml IFN- $\gamma$  at 33 °C. The differentiation was induced by IFN- $\gamma$ -free complete  $\alpha$ -MEM with 50  $\mu$ g/ml ascorbic acid and 4 mM  $\beta$ -glycerophosphate (differentiation media) at 37 °C with a medium change every other day. The murine monocyte cell line, RAW 264.7 was obtained from KAC Corporation (Kyoto, Japan) and maintained in complete  $\alpha$ -MEM. The murine pre-osteoblastic cell line, MC3T3-E1 was obtained from ATCC (Manassas, VA, USA) and maintained in complete  $\alpha$ -MEM.

All tissue culture reagents were from Gibco™/Life Technologies.

### Preparation and identification of extracellular vesicles

IDG-CM6 cells were cultured for 2 and 21 days in differentiation medium containing 5% FBS or EV-depleted FBS with a medium change every other day. The latter FBS was prepared using the FBS Exosome Depletion Kit I-Column Format (Norgen Biotek, Thorold, Canada). Following their differentiation, cells were cultured for another 2 days in normal medium containing EV-depleted FBS and the culture supernatant was collected. EVs were isolated from cell culture supernatants using Exoquick-TC™ (System Biosciences) as previously described.<sup>16</sup> The protein concentration of EVs was measured using the Protein Assay BCA Kit (FUJIFILM Wako Pure Chemical Corporation, Osaka, Japan). The ultrastructure of EVs was analyzed using transmission electron microscopy (TEM) as previously described.<sup>16</sup>

### Reverse transcription and real-time quantitative polymerase chain reaction (PCR)

Total RNA purification, complementary DNA preparation, and qPCR reactions were performed as previously described.<sup>16</sup> Murine glyceraldehyde 3-phosphate dehydrogenase (*Gapdh*) was used as an internal reference

control. PCR primer sequences for target genes are shown in Table 1.

### Western blotting

Immunodetection was conducted as previously described.<sup>16</sup> Briefly, whole-cell lysates or purified EVs were separated by sodium dodecyl sulfate-polyacrylamide gel electrophoresis, and then transferred to a polyvinylidene difluoride membrane (ATTO, Tokyo, Japan) for immunodetection with rabbit anti-exosome flotillin-1 (Cell Signaling Technology, Danvers, MA, USA) at 1:1000, mouse anti-CD63 (Biolegend, San Diego, CA, USA) at 1:1000, rabbit anti-calreticulin (Cell Signaling Technology) at 1:1000, rabbit anti-β-actin (Cell Signaling Technology) at 1:1000, or rabbit anti-TSG101 polyclonal (Novus Biologicals LLC, Centennial, CO, USA) at 1:500, and mouse anti-OCN (Takara Bio Inc., Shiga, Japan) at 1:200 as the primary antibodies.

### Uptake of EVs by RAW264.7 and MC3T3-E1 cells

Purified EVs were labeled with the PKH67 Green Fluorescent Cell Linker Kit® (Merck KGaA, Darmstadt, Germany) and incubated with cells for 6 and 24 h as previously described.<sup>16,19</sup> Nuclei were stained with Hoechst 33342 (Immunochemistry Technologies, Bloomington, MN, USA)

**Table 1** Primer sequences used for polymerase chain reaction amplifications.

Primer name	Direction	Sequence (5'-3')
<i>Dmp-1</i>	forward	CCACGTCTCTGAGGAAGACTA
	reverse	CTGCTTTCTGGGATGG
<i>Ctsk</i>	forward	TAGCACCCCTAGTCTTCCGC
	reverse	TTGAACACCCACATCCTGCT
<i>Oscar</i>	forward	TGCTGGTAACGGATCAGCTC
	reverse	AACAGTAGGTGCCAGGTGTG
<i>Acp5</i>	forward	TGAACCATGAGAAGTATGACAACA
	reverse	TATCTCCACATGTGTGAAGCCG
<i>Ocn</i>	forward	TGAACAGACTCCGGCG
	reverse	GATACCGTAGATGCGTTTG
<i>Bsp</i>	forward	GAGACGGCGATAGTTCC
	reverse	AGTGCCGCTAACTCAA
<i>Alp</i>	forward	GGGACATGCAGTATGAGTT
	reverse	GGCCTGGTAGTTGTTGTGAG
<i>Gapdh</i>	forward	AATGTGTCGGTCGTGGATCTGA
	reverse	GATGCTGCTTCAACACCTTCT

**Abbreviations:** Dentin matrix protein-1 (*Dmp-1*), Cathepsin-K (*Ctsk*), Osteoclast-associated receptor (*Oscar*), Acid-phosphatase5 (*Acp5*), Osteocalcin (*Ocn*), Bone sialoprotein (*Bsp*), Alkaline phosphatase (*Alp*), Glyceraldehyde-3-phosphate dehydrogenase (*Gapdh*).

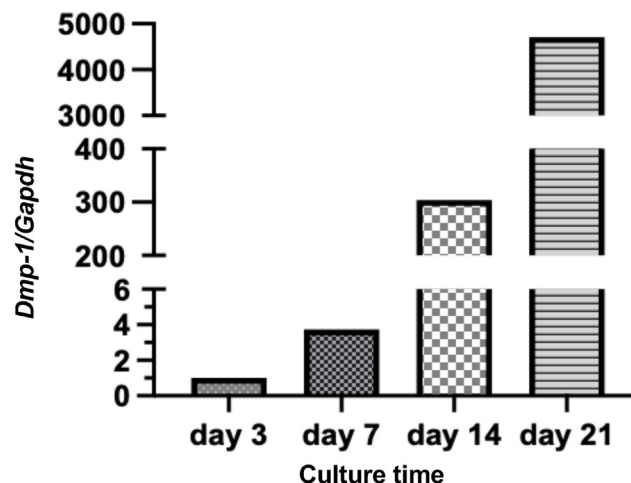


**Figure 1** Induction of the differentiation of IDG-CM6 cementocytes as an indicator of dentin matrix protein-1 expression.

Confluent monolayer cells were cultured in differentiation media containing 50 μg/ml ascorbic acid and 4 mM β-glycerophosphate for the indicated days with a medium change every other day. Total cellular RNA was extracted at the indicated time points and the gene expression of *Dmp-1* was analyzed by real-time PCR. Abbreviation: Dmp-1, dentin matrix protein-1.

for 5 min. Staining was evaluated by immunofluorescence microscopy.

### *In vitro* osteoclast formation assay

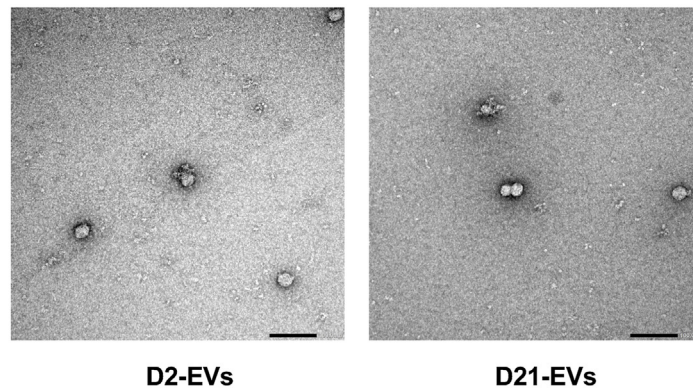
An osteoclast formation assay was conducted, as previously described.<sup>19</sup> Briefly, RAW 264.7 cells were cultured in the presence or absence of 50 ng/mL rRANKL in combination with 20  $\mu$ g/mL EVs or 50% (v/v) cell culture supernatants for 4 days in complete  $\alpha$ -MEM (0.5 mL/well). At the end of the culture period, cells were stained for tartrate-resistant acid phosphatase (TRAP) using a TRAP/ALP Stain Kit (FUJI-FILM Wako Pure Chemical Corporation), as previously described.<sup>19</sup> TRAP-positive osteoclasts were quantified by

counting the number of red-stained multinucleated ( $\geq 3$  nuclei) cells. Results are expressed as the number of TRAP-positive cells per well.

### Alkaline phosphatase (ALP) activity

ALP enzymatic activities were measured using p-nitrophenylphosphate as a substrate, as previously described.<sup>20</sup> Briefly, a confluent monolayer of MC3T3-E1 cells was lysed by repeating freezing and thawing three times and ALP enzymatic activities were measured. Absorbance was read spectrophotometrically at 405 nm. Enzyme activity is expressed as OD<sub>405</sub>/h.

**A**



**B**

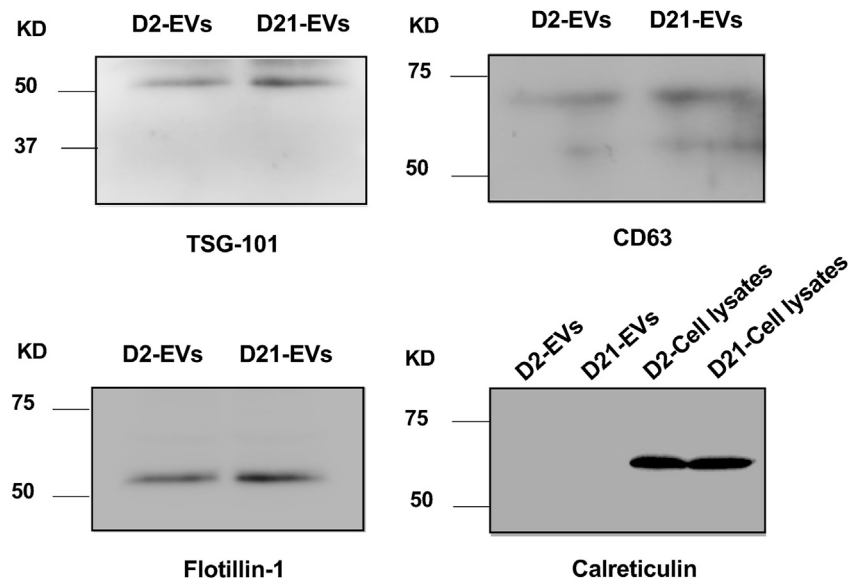


**Figure 2** Characterization of IDG-CM6 cementocyte-derived EVs.

(A): The morphology of EVs is shown by a TEM analysis. The left panel shows EVs extracted from D2-cementocytes (D2-EVs), and the right panel shows EVs extracted from D21-cementocytes (D21-EVs) (scale bars: 100 nm). (B): EVs and/or cell lysates were extracted from D2-cementocytes and D21-cementocytes, and Western blotting was performed using antibodies against the EV-related markers TSG101, CD63, and Flotillin-1 and the endoplasmic reticulum-related marker calreticulin. Abbreviation: EVs, extracellular vesicles.

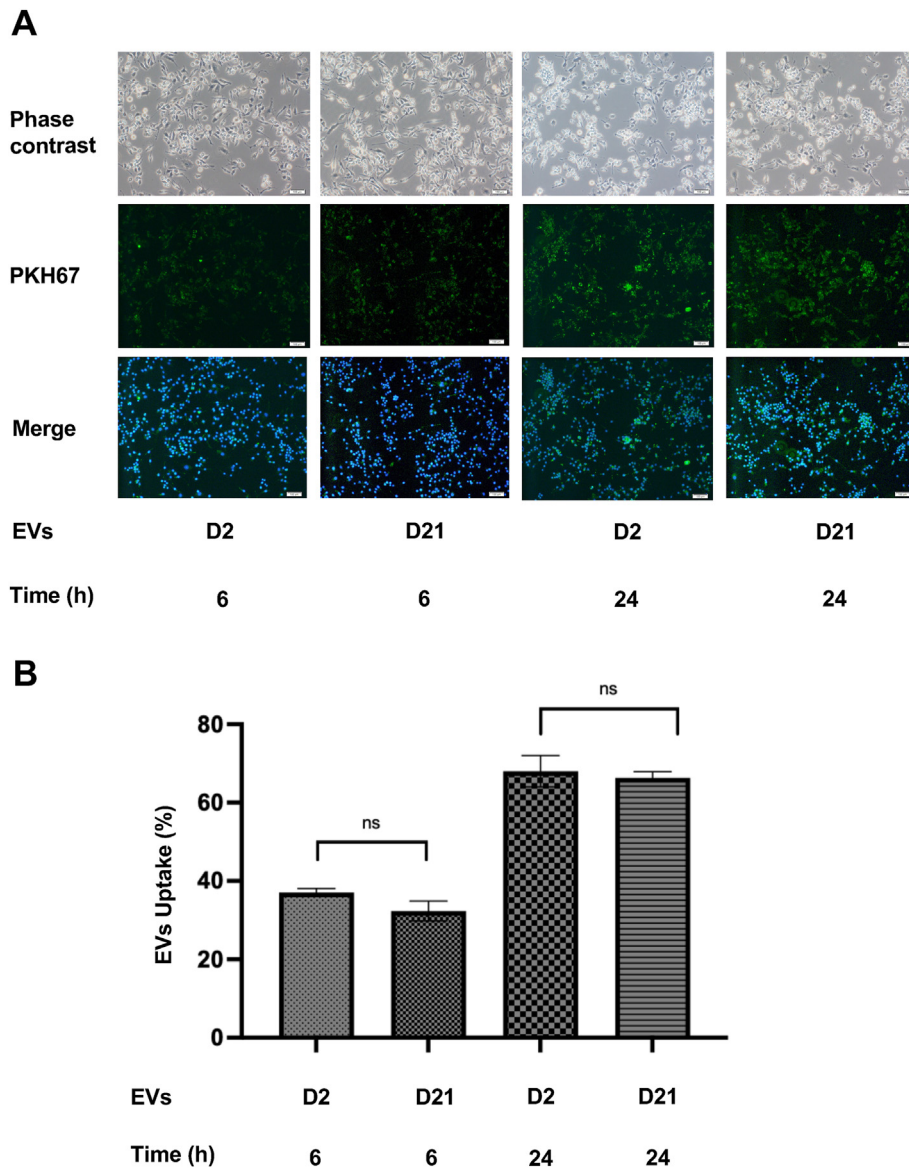


**Figure 3** Uptake of EVs by monocytes.

RAW 264.7 cells were incubated in the presence of PKH67-labeled EVs with 50 ng/ml rRANKL for 6 and 24 h. (A): Phase contrast is shown in the upper panels. EVs taken up by RAW 264.7 cells (light green in the middle panel) were detected by immunostaining after 6 and 24 h. Nuclei were visualized by staining with Hoechst 33342 (blue in the lower panel), and merged images are shown in the lower panel (scale bars: 100  $\mu$ m). (B): The number of cells stained with PKH67-labeled EVs was counted in three randomly selected fields (each containing  $\sim$ 100 cells). Representative data from three separate experiments are shown as the means  $\pm$  SE of triplicate assays. \*:  $P < 0.05$ .

### Statistical analysis

Differences between the control and experimental groups were evaluated by the Kruskal–Wallis test with the Steel post hoc test.  $P$  values  $< 0.05$  were regarded as significant.

### Results

#### Induction of IDG-CM6 cell differentiation using *dentin matrix protein-1* expression as an indicator

Cells were cultured in differentiation media for 21 days. The expression of *dentin matrix protein (Dmp)-1*, a marker gene

of the differentiation of cementocytes, was slightly increased by day 7, after which expression was strongly enhanced up to day 14 and further increased on day 21. In the present study, cells differentiated for 2 days (referred to as D2-cementocytes) and 21 days (referred to as D21-cementocytes) were used as early differentiated cementocytes and mature cementocytes, respectively (see Fig. 1).

#### Characterization of IDG-CM6 cell-derived extracellular vesicles

A TEM analysis showed the presence of EVs in the supernatants of D2- and D21-cementocytes, which were

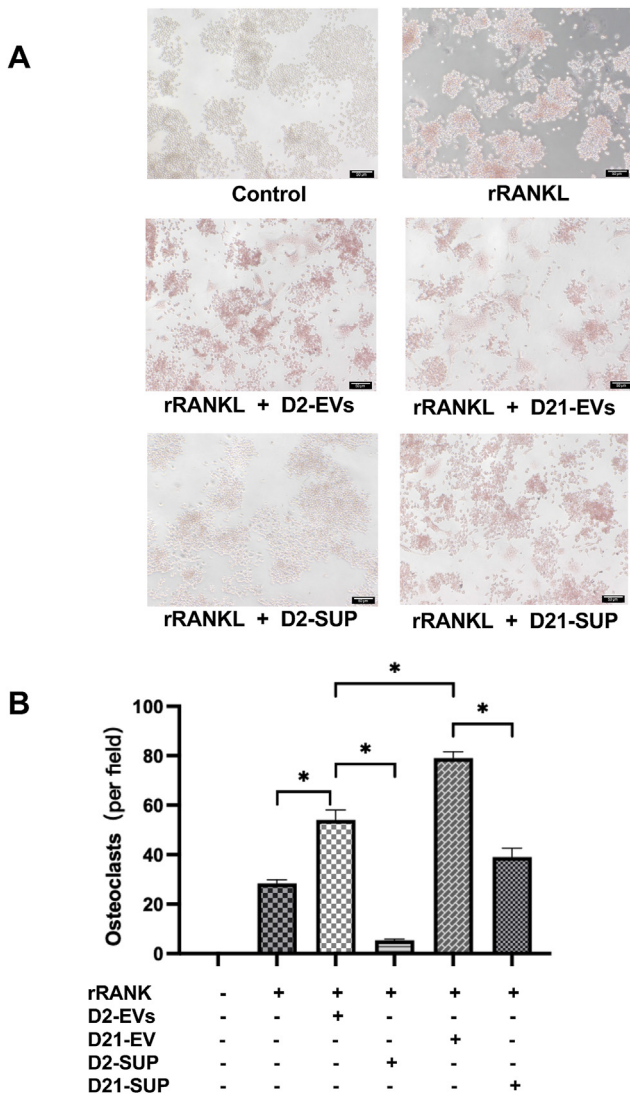


**Figure 4** Enhancing effects of EVs and inhibitory effects of supernatants on rRANKL-induced osteoclast formation.

RAW 264.7 cells were stimulated with or without rRANKL (50 ng/mL) for 5 days in the presence of 20  $\mu$ g/mL EVs from D2- and D21-cementocytes (referred to as D2-EVs and D21-EVs, respectively) or in the presence of culture supernatants from D2- and D21-cementocytes (referred to as D2-SUP and D21-SUP, respectively), and TRAP staining was performed. (A): The upper left panel shows the negative control and the upper right panel shows the positive control. The middle panels show the rRANKL stimulation group in the presence of each EV. The lower panels show the rRANKL stimulation group in the presence of each culture supernatant. The scale bar is 50  $\mu$ m. (B): The quantification of TRAP-positive osteoclasts shown in (A). Results are representative (A) or the mean  $\pm$  SE (B) of at least three independent experiments (\*:  $P < 0.05$ ). Abbreviation: rRANKL, recombinant receptor activator of nuclear factor- $\kappa$  B ligand.

characterized by a cup-shaped morphology and round membrane vesicles of approximately 50 nm in diameter, namely, typical EVs. No significant morphological differences were observed between EVs from each cementocyte

(Fig. 2A). A Western blot analysis (Fig. 2B) confirmed the expression of the EV-related markers, TSG101, CD63, and Flotillin-1 in each EV and the endoplasmic reticulum-associated (cytoplasmic) marker, calreticulin<sup>21</sup> in each cell lysate, but not in EVs.

### Enhancement of rRANKL-induced osteoclast formation by cementocyte-derived extracellular vesicles

We examined the effects of cementocyte-derived EVs on osteoclastogenesis. To verify that cementocyte-derived EVs were taken up by cells, PKH67-labeled EVs were cultured with RAW264.7 cells. An immunofluorescence microscopic analysis revealed that approximately 30–40% of EVs were detected on images of RAW264.7 cells 6 h after the addition of the EVs of D2- and D21-cementocytes, respectively, which increased further to approximately 70% after 24 h (Fig. 3A). The detection rate of EVs did not significantly differ between D2- and D21-cementocyte EVs (Fig. 3B). RAW264.7 cells were cultured with rRANKL in the presence of the EVs of D2- and D21-cementocytes. Fig. 4A and B showed a larger number of multinucleated osteoclasts and a higher intensity of TRAP staining than in the rRANKL alone group. This enhancing effect was significantly more potent for D21-cementocyte-derived EVs than for D2-cementocyte-derived EVs. Fig. 5 showed that the gene expression levels of osteoclast-related molecules, i.e., *Ctsk*, *Oscar*, and *Acp5*, were significantly higher than those in the rRANKL alone group; however, no significant differences were observed between the D2- and D21-cementocyte groups. These results suggest that EVs exerted an enhancing effect on osteoclast differentiation that was more potent for well-differentiated cementocyte-derived EVs.

### Inhibition of rRANKL-induced osteoclastogenesis by cementocyte-derived supernatants

Since supernatants contain various biologically active factors as well as EVs, the effects of supernatants on osteoclastogenesis were investigated. RAW264.7 cells were cultured in rRANKL for 5 days in the presence of D2- or D21-cementocyte derived-supernatants, both of which theoretically contained about 20  $\mu$ g/mL of EVs, and osteoclast formation was analyzed by TRAP staining. As shown in Fig. 4A (panels in the third row) and 4B, the formation of TRAP-positive multinucleated osteoclasts was more strongly suppressed in the D2- and D21-supernatant groups. These results indicate that cementocytes simultaneously produced soluble factors that neutralized EV-mediated osteoclastogenesis.

### Inhibition of recombinant bone morphogenetic protein-2 induced osteoblast differentiation by cementocyte-derived extracellular vesicles

We examined the effects of cementocyte-derived EVs on the regulation of rBMP-2-induced osteoblast differentiation. To verify that cementocyte-derived EVs were taken up

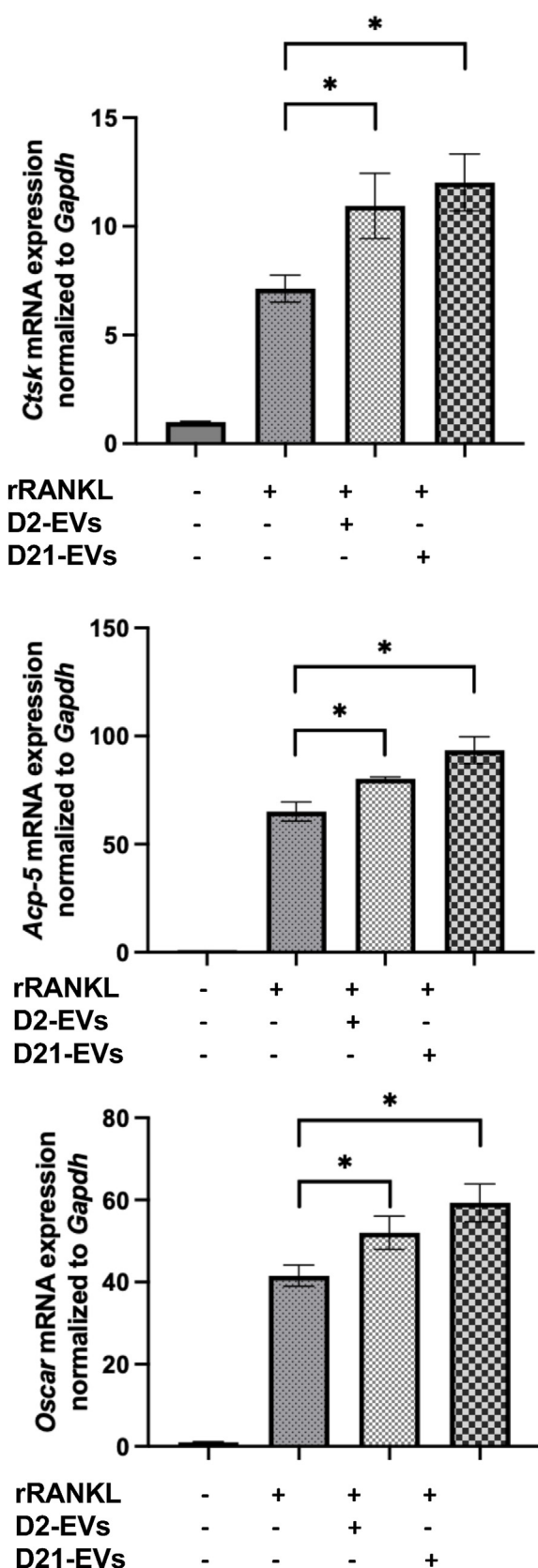


**Figure 5** Enhancing effects of EVs on rRANKL-induced osteoclast-related molecules at the gene level. RAW 264.7 cells were stimulated with or without rRANKL (50 ng/mL) for 3 days in the presence of 20 µg/mL EVs from D2-

by cells, PKH67-labeled EVs were cultured with MC3T3-E1 cells, a mouse pre-osteoblast cell line. Fig. 6A and B shows that approximately 40% of EVs were detected on images of MC3T3-E1 cells 6 h after the addition of EVs, and most cells showed fluorescence at 24 h in D2- and D21-cementocytes. MC3T3-E1 cells were cultured with rBMP-2 in the presence of the EVs of D2- and D21-cementocytes and ALP enzymatic activity was measured. Fig. 7A shows that the addition of the EVs of D2- and D21-cementocytes significantly inhibited rBMP-2-induced ALP activity, and this effect was significantly stronger in the EVs of D21-cementocytes than in those of D2-cementocytes. On the other hand, the EVs of neither D2- nor D21-cementocytes exerted a significant effect on ALP activity induced by Wnt3a, a representative canonical Wnt ligand (Fig. 7B and C). Osteoblast differentiation molecules, such as the OCN and BSP genes, were significantly suppressed by the EVs of D2- and D21-cementocytes (Fig. 8A). At the protein level, the expression of OCN was significantly suppressed by the respective EVs (Fig. 8B and C). The inhibitory effects of EVs were significantly stronger for those derived from D21-cementocytes than from D2-cementocytes. These results suggest that EVs secreted from cementocytes exerted inhibitory effects on rBMP-2-induced osteoblast differentiation, and these effects were more potent for EVs from well-differentiated cementocytes.

### Discussion

The present study suggests the presence of a network of cementocytes, osteoblasts, and osteoclasts in cementum and the involvement of cementocytes in dynamic metabolism of cementum.

Cementum is generally assumed to have a very limited capacity for remodeling and is resistant to resorption by osteoclasts. Furthermore, clinical findings showed that cementum is rarely absorbed even under conditions in which osteoclasts resorb alveolar bone, such as severe periodontitis. Previous *in vitro* studies that focused on cementoblasts revealed that osteoprotegerin (OPG) was constitutively synthesized and secreted in contrast to low levels of RANKL expression.<sup>22,23</sup> Recent studies using the extracted tissue of experimental animals also reported higher OPG and lower RANKL levels in cellular cementum than in long bones and alveolar bone.<sup>24</sup> In addition, *in vitro* studies that focused on cementocytes revealed that when cementocytes were cultured under fluid flow shear stress, the OPG/RANKL ratio increased, and was approximately 40-fold higher than that of osteocytes under the same conditions.<sup>24</sup> Based on these findings, the present result showing that the culture supernatant of cementocytes abrogated rRANKL-induced osteoclastogenesis may be due to secreted OPG in the supernatant although further study using neutralizing antibody or siRNA against OPG need to be

and D21-cementocytes. Total cellular RNA was extracted and the gene expression of *Cathepsin-K (Ctsk)*, *acidphosphatase5 (Acp5)*, and *osteoclast-associated receptor (Oscar)* were analyzed by real-time PCR. Representative findings of three independent experiments are shown (\*:  $P < 0.05$ ).

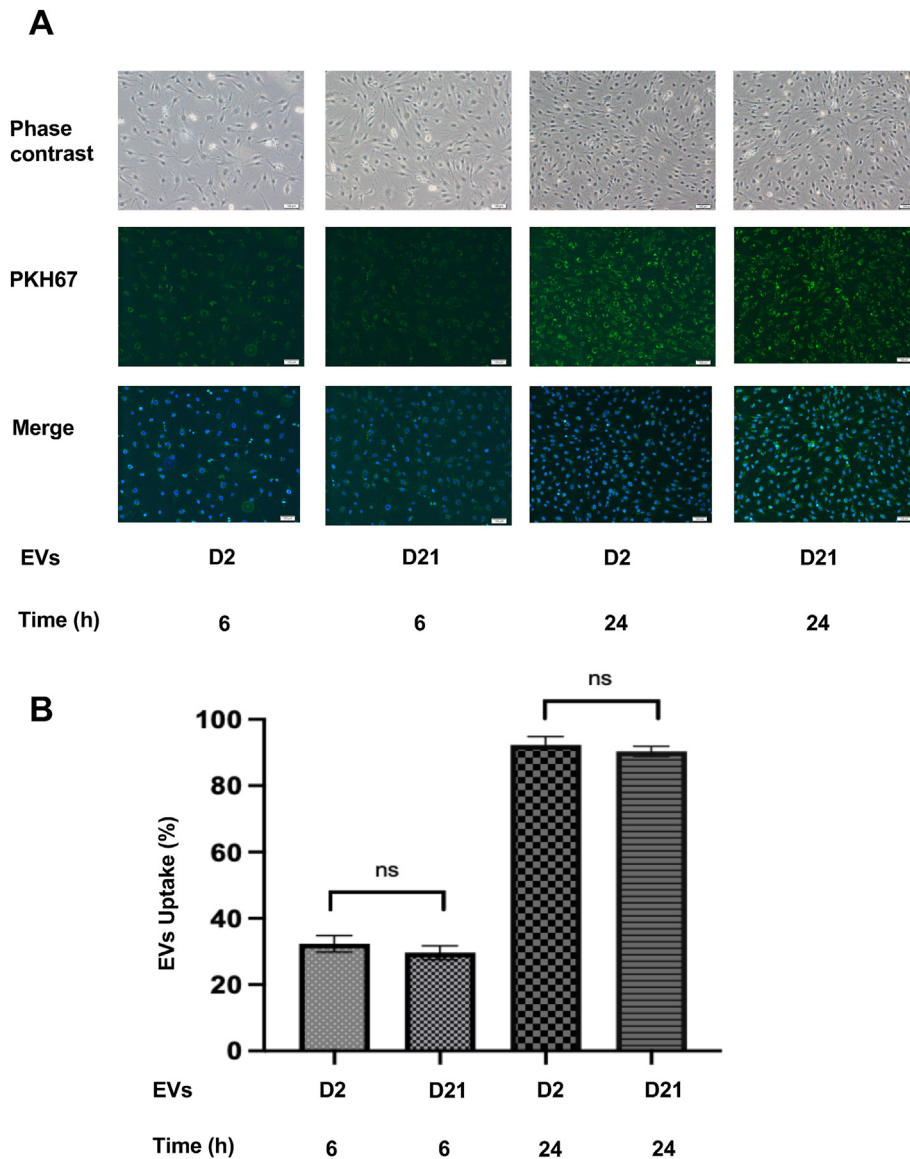


**Figure 6** Uptake of EVs by pre-osteoblasts.

The mouse pre-osteoblast cell line, MC3T3-E1 was incubated in the presence of PKH67-labeled EVs with or without 100 ng/ml rBMP-2 for 6 and 24 h. (A): Phase contrast images are shown in the upper panels. EVs taken up by MC3T3-E1 cells were detected by immunostaining after 6 and 24 h (light green in the middle panel). Nuclei were visualized by staining with Hoechst 33342 (blue in the lower panel), and merged images are shown in the lower panel (scale bars: 100  $\mu$ m). (B): The number of cells stained with PKH67-labeled EVs was counted in three randomly selected fields (each containing  $\sim$ 100 cells). Representative data from three separate experiments are shown as the means  $\pm$  SE of triplicate assays. \*:  $P < 0.05$ , ns: not significant.

conducted. While, the resorption of cementum is often observed at the site of lesions due to trauma, orthodontics, or pathological stimuli, such as large apical periodontitis.<sup>25</sup> Previous studies demonstrated that cementoblasts produced chemotactic factors for osteoclast progenitors when stimulated with *P. gingivalis* lipopolysaccharide,<sup>23</sup> and also that the OPG/RANKL ratio was reduced by a stimulation with IL-1 $\beta$  or with sclerostin.<sup>26,27</sup> We also recently reported that EVs secreted from OCCM-30 cells, a mouse cementoblast cell line, enhanced the formation of rRANKL-induced osteoclasts.<sup>19</sup> The present study showed that cementocyte-derived EVs enhanced the formation of osteoclasts, suggesting the presence of a network of

cementocytes and osteoclasts in cellular cementum and that cementocytes may be involved in dynamic metabolism of cellular cementum through cytokines, signaling molecules, and EVs.

BMP-2 has a potent osteogenic differentiation potential.<sup>28</sup> When BMP-2 was administered directly to a periodontal tissue defect in animal models, the periodontal ligament and cementum rarely formed and it induced ankylosis, with alveolar bone and cementum adhering together.<sup>29,30</sup> On the other hand, Wnts are a family of secreted glycoproteins that regulate developmental and post-developmental functions.<sup>31</sup> The canonical Wnt pathway, represented by Wnt3a, is primarily involved in



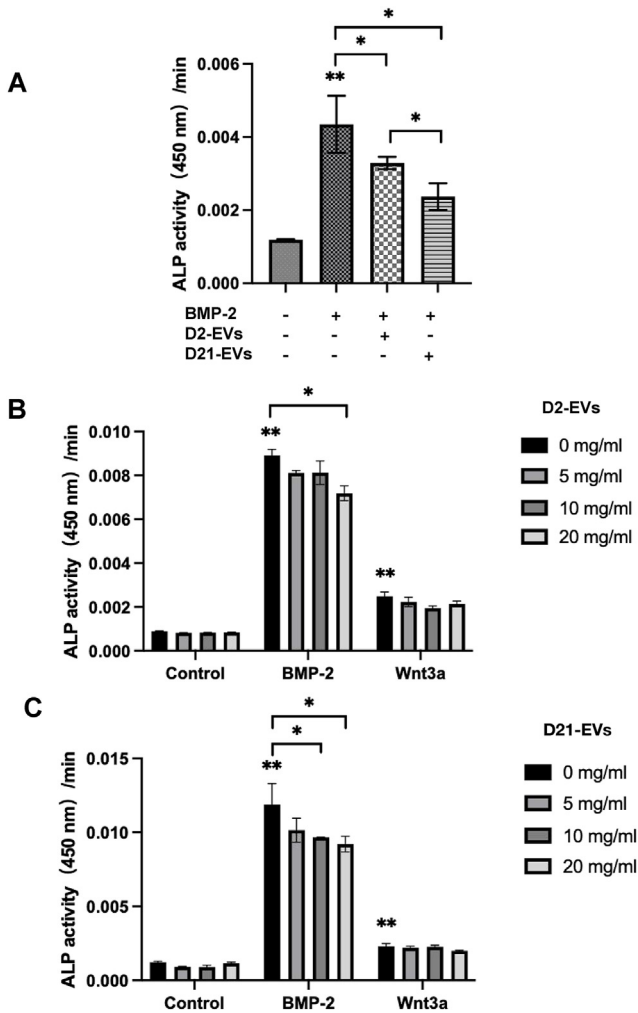


**Figure 7** Inhibitory effects of cementocyte-derived EVs on bone morphogenetic protein (rBMP)-2-induced alkaline phosphatase (ALP) activity. MC3T3-E1 cells were stimulated with 100 ng/ml rBMP-2 for 5 days in the presence of 20  $\mu$ g/ml EVs from D2- and D21-cementocytes (A). MC3T3-E1 cells were stimulated with 100 ng/ml rBMP-2 or 30 ng/ml rmWnt3a for 5 days in the presence of various concentrations of EVs from D2-cementocytes (B) or D21-cementocytes (C). ALP activity for whole-cell lysates was measured as described in the Materials and Methods. Representative data from three separate experiments are shown as the means  $\pm$  SE of triplicate assays. The significance of differences is shown (\*\* $P < 0.05$  vs. untreated cells, \* $P < 0.05$  between the indicated groups).

bone formation.<sup>32</sup> Numerous studies showed that Wnt signals are important for maintaining periodontal tissue homeostasis.<sup>33,34</sup> Pathological root resorption may be associated with reduced endogenous Wnt signaling.<sup>33</sup> In the present study, EVs did not significantly affect Wnt3a-induced ALP expression. Based on previous findings on BMP-2 and Wnt, the present results, namely, the selective inhibitory effect of cementocyte-derived EVs on the rBMP2 stimulation, suggest the involvement of EVs in maintaining periodontal tissue homeostasis.

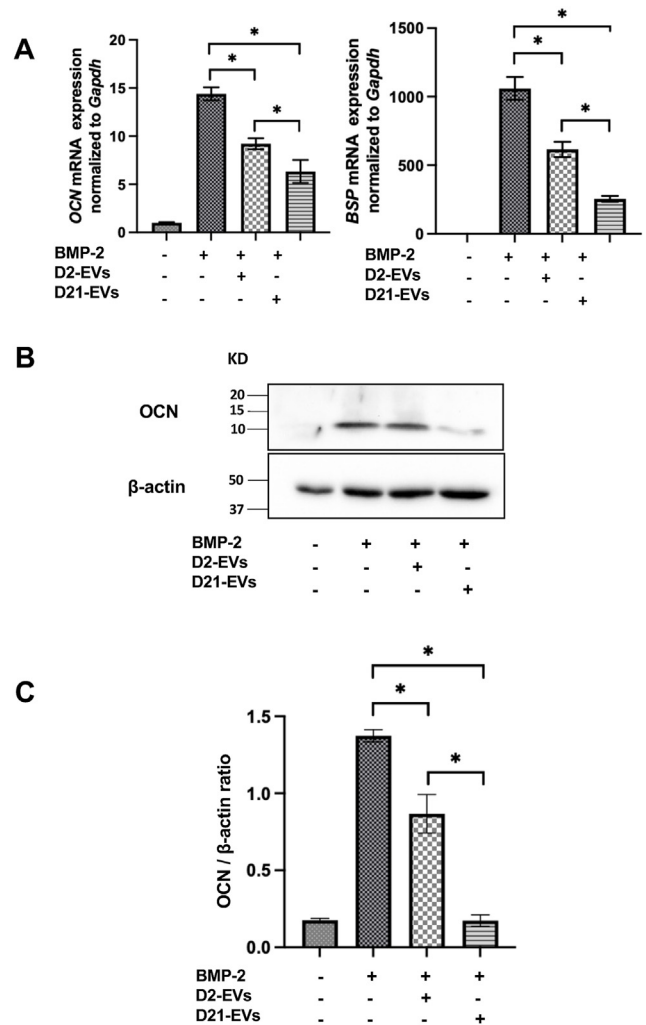


**Figure 8** Inhibitory effects of cementocyte-derived EVs on rBMP-2-induced osteoblast-related molecules. MC3T3-E1 cells were stimulated with 100 ng/ml rBMP-2 for 5 days in the presence of 20  $\mu$ g/ml EVs from D2- and D21-cementocytes. (A): Total cellular RNA was extracted and the gene expression of *Ocn* and *Bsp* was analyzed by real-time PCR. (B): Cell lysates were extracted and a Western blotting analysis using the OCN antibody was performed with  $\beta$ -actin as the reference protein. (C): The expression level of OCN was quantified via densitometry scanning. The relative expression level of OCN normalized to  $\beta$ -actin. Representative findings of three independent experiments are shown as the means  $\pm$  SE of triplicate assays. \*:  $P < 0.05$ . Abbreviations: OCN, osteocalcin, BSP, bone sialoprotein.

Among the signaling molecules of EVs, miRNAs have been shown to be an important mechanism for the functions of EV.<sup>35</sup> It has been reported that osteoclastogenesis induced is enhanced by several miRNAs,<sup>36</sup> including miR-148a<sup>37</sup> and miR-214.<sup>38</sup> In addition, miR-218<sup>39</sup> and miR-124-3p<sup>40</sup> of osteocyte EVs have been reported to inhibit osteoblast differentiation. Future research will be needed to analyze the expression of miRNAs in EVs from cementocytes.

The present study demonstrated that EVs in cementocytes regulate osteoclasts and osteoblasts, and further

studies will not only provide insights into the mechanisms maintaining periodontal tissue homeostasis, but will also lead to the development of therapies for root resorption and ankylosis.

## Declaration of competing interest

The authors have no conflicts of interest to declare related to the present study.

## Acknowledgments

This study was supported by a Grant-in-Aid for JSPS KAKENHI (23K09163).

## References

- Foster BL, Somerman MJ. Cementum. In: McCauley LK, Somerman MJ, eds. *Mineralized tissues in oral and craniofacial science*. Iowa: A John Wiley & Sons Inc, 2012:169–82.
- Bosshardt DD. Are cementoblasts a subpopulation of osteoblasts or a unique phenotype? *J Dent Res* 2005;84:390–406.
- Dallas SL, Prideaux M, Bonewald LF, et al. The osteocyte: an endocrine cell and more. *Endocr Rev* 2013;34:658–90.
- Bonewald LF. The amazing osteocyte. *J Bone Miner Res* 2011;26:229–38.
- Ayasaka N, Kondo T, Goto T, et al. Differences in the transport systems between cementocytes and osteocytes in rats using microperoxidase as a tracer. *Arch Oral Biol* 1992;37:363–9.
- Kagayama M, Sasano Y, Mizoguchi I, et al. Confocal microscopy of cementocytes and their lacunae and canaliculi in rat molars. *Anat Embryol* 1997;195:491–6.
- Hirashima S, Ohta K, Kanazawa T, et al. Cellular network across cementum and periodontal ligament elucidated by FIB/SEM tomography. *Microscopy (Oxf)* 2020;69:53–8.
- Camussi G, Derigibus MC, Bruno S, et al. Exosomes/microvesicles as a mechanism of cell-to-cell communication. *Kidney Int* 2010;78:838–48.
- Barile L, Moccetti T, Marbán E, et al. Roles of exosomes in cardioprotection. *Eur Heart J* 2017;38:1372–9.
- Haj-Salem I, Plante S, Gounni AS, et al. Fibroblast-derived exosomes promote epithelial cell proliferation through TGF- $\beta$ 2 signalling pathway in severe asthma. *Allergy* 2018;73:178–86.
- Cui Y, Luan J, Li H, et al. Exosomes derived from mineralizing osteoblasts promote ST2 cell osteogenic differentiation by alteration of microRNA expression. *FEBS Lett* 2016;590:185–92.
- Deng L, Wang Y, Peng Y, et al. Osteoblast-derived microvesicles: a novel mechanism for communication between osteoblasts and osteoclasts. *Bone* 2015;79:37–42.
- Lamichhane TN, Sokic S, Schardt JS, et al. Emerging roles for extracellular vesicles in tissue engineering and regenerative medicine. *Tissue Eng Part B Rev* 2015;21:45–54.
- Zhang Y, Liu F, Yuan Y, et al. Inflammasome-derived exosomes activate NF- $\kappa$ B signaling in macrophages. *J Proteome Res* 2017;16:170–8.
- Ni H, Yang S, Siaw-Debrah F, et al. Exosomes derived from bone mesenchymal stem cells ameliorate early inflammatory responses following traumatic brain injury. *Front Neurosci* 2019;13:14.
- Wang Z, Maruyama K, Sakisaka Y, et al. Cyclic stretch force induces periodontal ligament cells to secrete exosomes that suppress IL-1 $\beta$  production through the inhibition of the NF- $\kappa$ B signaling pathway in macrophages. *Front Immunol* 2019;10:1310.
- Lv PY, Gao PF, Tian GJ, et al. Osteocyte-derived exosomes induced by mechanical strain promote human periodontal ligament stem cell proliferation and osteogenic differentiation via the miR-181b-5p/PTEN/AKT signaling pathway. *Stem Cell Res Ther* 2020;11:295.
- Nakao Y, Fukuda T, Zhang Q, et al. Exosomes from TNF- $\alpha$ -treated human gingiva-derived MSCs enhance M2 macrophage polarization and inhibit periodontal bone loss. *Acta Biomater* 2021;122:306–24.
- Sato R, Maruyama K, Nemoto E, et al. Extracellular vesicles derived from murine cementoblasts possess the potential to increase RANKL-induced osteoclastogenesis. *Front Physiol* 2022;13:825596.
- Nemoto E, Sakisaka Y, Tsuchiya M, et al. Wnt3a signaling induces murine dental follicle cells to differentiate into cementoblastic/osteoblastic cells via an osterix-dependent pathway. *J Periodontol Res* 2016;51:164–74.
- Rosenberger L, Ezquer M, Lillo-Vera F, et al. Stem cell exosomes inhibit angiogenesis and tumor growth of oral squamous cell carcinoma. *Sci Rep* 2019;9:663.
- Boabaid F, Berry JE, Koh AJ, et al. The role of parathyroid hormone-related protein in the regulation of osteoclastogenesis by cementoblasts. *J Periodontol* 2004;75:1247–54.
- Nemoto E, Darveau RP, Foster BL, et al. Regulation of cementoblast function by P. gingivalis lipopolysaccharide via TLR2. *J Dent Res* 2006;85:733–8.
- Zhao Jr N, Nociti FH, Duan P, et al. Isolation and functional analysis of an immortalized murine cementocyte cell line, IDG-CM6. *J Bone Miner Res* 2016;31:430–42.
- Feller L, Khammissa RA, Thomadakis G, et al. Apical external root resorption and repair in orthodontic tooth movement: biological events. *BioMed Res Int* 2016;2016:4864195.
- Huynh NC, Everts V, Pavaasant P, et al. Interleukin-1 $\beta$  induces human cementoblasts to support osteoclastogenesis. *Int J Oral Sci* 2017;9:e5.
- Bao X, Liu Y, Han G, Zuo Z, Hu M. The effect on proliferation and differentiation of cementoblast by using sclerostin as inhibitor. *Int J Mol Sci* 2013;14:21140–52.
- Ducy P, Karsenty G. The family of bone morphogenetic proteins. *Kidney Int* 2000;57:2207–14.
- Wikesjö UM, Guglielmoni P, Promsudthi A, et al. Periodontal repair in dogs: effect of rhBMP-2 concentration on regeneration of alveolar bone and periodontal attachment. *J Clin Periodontol* 1999;26:392–400.
- Takahashi D, Odajima T, Morita M, et al. Formation and resolution of ankylosis under application of recombinant human bone morphogenetic protein-2 (rhBMP-2) to class III furcation defects in cats. *J Periodontol Res* 2005;40:299–305.
- Logan CY, Nusse R. The Wnt signaling pathway in development and disease. *Annu Rev Cell Dev Biol* 2004;20:781–810.
- Krishnan V, Bryant HU, Macdougald OA. Regulation of bone mass by Wnt signaling. *J Clin Invest* 2006;116:1202–9.
- Lim WH, Liu B, Hunter DJ, et al. Downregulation of Wnt causes root resorption. *Am J Orthod Dentofacial Orthop* 2014;146:337–45.
- Lim WH, Liu B, Mah S, et al. Alveolar bone turnover and periodontal ligament width are controlled by Wnt. *J Periodontol* 2015;86:319–26.
- Huang X, Xiong X, Liu J, Zhao Z, Cen X. MicroRNAs-containing extracellular vesicles in bone remodeling: an emerging frontier. *Life Sci* 2020;254:117809.

36. Franceschetti T, Dole NS, Kessler CB, Lee SK, Delany AM. Pathway analysis of microRNA expression profile during murine osteoclastogenesis. *PLoS One* 2014;9:e107262.
37. Cheng P, Chen C, He HB, et al. miR-148a regulates osteoclastogenesis by targeting V-maf musculoaponeurotic fibrosarcoma oncogene homolog B. *J Bone Miner Res* 2013;28:1180–90.
38. Zhao C, Sun W, Zhang P, et al. miR-214 promotes osteoclastogenesis by targeting Pten/PI3k/Akt pathway. *RNA Biol* 2015;12:343–53.
39. Qin Y, Peng Y, Zhao W, et al. Myostatin inhibits osteoblastic differentiation by suppressing osteocyte-derived exosomal microRNA-218: a novel mechanism in muscle-bone communication. *J Biol Chem* 2017;292:11021–33.
40. Li J, Guo Y, Chen YY, et al. miR-124-3p increases in high glucose induced osteocyte-derived exosomes and regulates galectin-3 expression: a possible mechanism in bone remodeling alteration in diabetic periodontitis. *Faseb J* 2020;34:14234–49.